1   **Wastewater characterisation by combining size fractionation, chemical composition and**

2   **biodegradability**

3

4   Kristin T. Ravndal[a,b], Eystein Opsahl[a], Andrea Bagi[a,c] and Roald Kommedal[a,*]

5   [a] University of Stavanger, Department of Mathematics and Natural Science, 4036 Stavanger,

6   Norway

7   [b] Cranfield Water Science Institute, Cranfield University, Bedfordshire, MK43 0AL, UK

8   [c] Marine Environment Group, International Research Institute of Stavanger, Mekjarvik 12,

9   4070 Randaberg, Norway

10

11

12

13   * Corresponding author: roald.kommedal@uis.no

14

15   Submitted to Water research on 30. September 2017

16

Abstract

The potential for resource recovery from wastewater can be evaluated based on a detailed characterisation of wastewater. In this paper, results from fractionation and characterisation of two distinct wastewaters are reported. Using tangential flow filtration, the wastewater was fractionated into 10 size fractions ranging from 1 kDa to 1 mm, wherein the chemical composition and biodegradability were determined. Carbohydrates were dominant in particulate size fractions larger than 100 µm, indicating a potential of cellulose recovery from these fractions. While the particulate size fractions between 0.65-100 µm show a potential as a source for biofuel production due to an abundance of saturated C16 and C18 lipids. Both wastewaters were dominated by particulate (>0.65 µm), and oligo- and monomeric (<1 kDa) COD. Polymeric (1-1000 kDa) and colloidal (1000 kDa-0.65 µm) fractions had a low COD content, expected due to degradation in the sewer system upstream of the wastewater treatment plant. Biodegradation rates of particulate fractions increase with decreasing size. However, this was not seen in polymeric fractions where degradation rate was governed by chemical composition. Analytical validation of molecular weight and particle size distribution showed below filter cut-off retention of particles and polymers close to nominal cut-off, shifting the actual size distribution.

34 # Keywords

35 Wastewater fractionation

36 Wastewater characterization

37 Resource recovery

38 Biodegradability

39

40 # Abbreviations

41 BOD: Biological oxygen demand

42 COD: Chemical oxygen demand

43 COD/TN-ratio: COD to total nitrogen ratio

44 COD/TP-ratio: COD to total phosphorous ratio

45 MALS: Multi angle light scattering detector

46 OM: Organic matter

47 p.e: Person equivalents

48 PSD: Particle size distribution

49 SEC: Size exclusion chromatography

50 TSS: Total suspended solids

51 VSS: Volatile suspended solids

52 WWTP: Wastewater treatment plant

1 Introduction

Wastewater treatment has over the last century effectively improved recipient water quality, reduced water pathogenicity and improved human health (van Loosdrecht and Brdjanovic, 2014). Being primarily concerned with water and sludge quality prior to disposal, attention has been on removal mechanisms and unit processes for that purpose (Wilsenach et al., 2003). Freshwater shortage in arid regions stimulated research and development of technologies for reuse of treated wastewater (Asano and Levine, 1998). Energy and nutrient recovery has gradually been integrated with treatment, and the last decades have seen increased attention on both improved recovery and energy efficiency (Verstraete et al., 2009). More recently, wastewater is seen as an important resource for bio-based production in circular waste management (Puyol et al., 2017; Wang et al., 2015). This calls for future wastewater technologies that recover wastewater valuables, in addition to nutrient, energy and water reclamation (Puchongkawarin et al., 2015). Among putative technologies includes membrane based up-concentration (Verstraete et al., 2009), intensified and integrated distillation (Harmsen, 2007), advanced biological conversion and absorption (Matassa et al., 2015; Puyol et al., 2017) and mixed culture solvent extraction (Wahlen et al., 2011).

Characterisation of physical and chemical components in wastewater is a prerequisite for design and operation of wastewater treatment processes. Molecular and particulate size distributions of components are important for evaluation of degradation and removal mechanisms, and was first combined by Levine et al. (1991). As novel process technologies and formulation of next generation treatment objectives for resource recovery will target more specific compounds in raw wastewater, more detailed characterization is required (Choubert et al., 2013; Tran et al., 2015). Compared to current characterisation strategies (e.g. the STOWA approach; see review by Roeleveld and Van Loosdrecht, 2002), details on chemical composition and biodegradability of size classes is necessary.

78 Traditionally, organic matter (OM) in wastewater has been fractionated into four size

79 fractions (Levine et al., 1991), however, the use of micro- and ultrafiltration allowed for

80 further separation of dissolved and colloidal size fractions in later studies (Dulekgurgen et al.,

81 2006; Karahan et al., 2008; Sophonsiri and Morgenroth, 2004). A few researchers have

82 combined size fractionation either with chemical composition (Sophonsiri and Morgenroth,

83 2004) or biodegradability (Karahan et al., 2008). However, these studies do not combine all

84 three factors. In addition, none of these studies validated the actual size distribution of the

85 obtained fractions, a concern related to known bias effects in ultra- and nanofiltration

86 (Cheryan, 1998). Hence, there is a need to evaluate wastewater components by the

87 combination of a validated size fractionation, with both chemical composition and

88 biodegradability of all size fractions.

89 The objectives of this study were to i) separate wastewater into several size fractions from

90 below 1 kDa to above 1 mm and validate the size distribution of the fractions analytically, ii)

91 quantitatively characterize the fractions in terms of nutritional and macromolecular

92 composition, iii) determine the biodegradability and evaluate which factors affect

93 biodegradation in each size range, and iv) evaluate the potential for resource recovery based

94 on the detailed composition analysis performed.

95 ## 2   Materials and Methods

96 Wastewater samples were collected from two wastewater treatment plants (WWTP) located in

97 south-west Norway. Vik WWTP (approx. 50000 p.e.) receives wastewater from households in

98 the Jæren region, with significant contributions from agriculture and food processing

99 industries. Mekjarvik WWTP (approx. 250000 p.e) is located downstream of the urban areas

100 of Stavanger and Sandnes, and receive mainly domestic wastewater with some contribution

101 from small-scale service industries. Hence, the two wastewaters investigated here represent

102 (1) a high strength (especially in terms of COD) wastewater with dominant industrial loading

103 (Vik) and (2) a typical low to intermediate strength municipal wastewater (Mekjarvik).

104 2.1   Wastewater sampling and fractionation

105 At Vik WWTP, a 50 L screened (6 mm) raw wastewater grab-sample was collected in the

106 morning. At Mekjarvik WWTP, 60 L of wastewater was collected by a flow proportional

107 automatic composite sampler over 20 hours (Contronics PSW 2000). Immediately upon

108 arrival to the lab, pH of the wastewater sample was lowered to below 2.3 with concentrated

109 hydrochloric acid and kept refrigerated at 2 °C to prevent biodegradation during storage. Size

110 fractionation was carried out upon arrival by serial sieving, and cross flow micro- and

111 ultrafiltration as described in the supplementary information. Sieving was performed using

112 stainless steel sieves (VWR collection) with nominal sieve mesh sizes of 1 mm, 100 µm and

113 25 µm. Followed by serial microfiltration and ultrafiltration using a Cogent M1 tangential

114 flow filtering system (Merck Millipore). Microfiltration modules used were 0.65 µm and 0.1

115 µm Pellicon 2 Durapore C-screen filters 0.1 m^2 (Merck Millipore), while ultrafiltration were

116 performed using 1000 kDa, 100 kDa and 10 kDa Pellicon 2 Ultracel C-screen filter cassettes

117 0.1 m^2 (Merck Millipore), and 1 kDa Pellicon 2 Mini Ultrafiltration Module C-screen 0.1 m^2

118 (Merck Millipore).

119 2.2   Validation of size distribution

120 2.2.1   Particle size distribution

121 Particle size distributions (PSD) of the 100-1000 µm, 25-100 µm and 0.65-25 µm fractions

122 were analysed by a Multisizer 4 coulter counter (Beckman Coulter) using a 1000 µm aperture

123 tube (measuring range 25-600 µm), a 200 µm aperture tube (measurement range 4-120 µm)

124 and a 100 µm aperture tube (2-60 µm) for the respective size fractions. For 200 and 100 µm

125 aperture tubes, 0.9 M% NaCl was used as electrolyte, while for the largest fraction, a mixture

126 of 0.9 M% NaCl (60 V%) and glycerol (40 V%) was used. Depending on the particle

127   concentration, 0.1-1 mL sample was diluted to 200 mL with corresponding electrolyte for all

128   analysis. Electrolyte blanks were measured for background noise subtraction.

129   2.2.2   Molecular weight and rms-radius

130   Molecular weight and rms-radius distribution of polymeric and colloidal fractions were

131   measured using an Agilent 1260 Infinity HPLC connected to multi angle light scattering

132   (MALS) detector (Dawn Heleos II 18, Wyatt Technology) and a differential refractive index

133   detector (Waters 2410). The HPLC system was equipped with a Shodex OHpak SB-807 HQ

134   column, a SB-805 HQ column (with additional SB-803 HQ column for the lower fractions)

135   and a OHpak SB-807G guard column, all kept at 20 °C throughout the experiment. Sodium

136   azide (0.1 g L^{-1}) fixated concentrated fraction samples were filtered through either 1.2 μm or

137   0.45 μm cellulose nitrate syringe filters, depending on fraction size, and 100 μL was injected

138   into an isocratic mobile phase flow of 0.5 mL min^{-1}. The mobile phase was prepared by

139   filtering an aqueous buffer solution containing 13.4 g L^{-1} Na-HEPES (Sigma-Aldrich), 0.625

140   g L^{-1} HNO_3 (Sigma-Aldrich), 8.5 g L^{-1} $NaNO_3$ (Sigma-Aldrich), and 0.1 g L^{-1} sodium azide

141   (Sigma-Aldrich) through a 0.1 µm filter (Millipore - Durapore). Sample run time was set to

142   90 minutes with total elution time of roughly 45 minutes, to allow re-equilibration of the

143   columns. The injection needle was flushed between each injection to limit cross

144   contamination. A bovine serum albumin (BSA) standard (0.5 g L^-, 0.185 mL g^{-1}, 66 kDa) was

145   used as a control with regards to normalization, alignment, band broadening and for

146   verification of the method in general. A dn/dc value of 0.165 was used as it approximate the

147   average value for heterogeneous biopolymers (Cheong et al., 2015; Zhao et al., 2011). The

148   ASTRA 6.0 software (Wyatt Technology, 2017) was used for data interpretation using a

149   Berry 1st degree fit for all fractions. Detectors 8 through 18 were enabled for molecular

150   weight analysis, while detectors 3 through 18 were enabled for the determination of rms

151   radius of fractions larger than 100 kDa. MALS data was extrapolated at low peak-end of

152 fractions smaller than 10 kDa, while dRI data was extrapolated on high peak-end of fractions

153 larger than 100 kDa.

154 ## 2.3 Solids and chemical composition analysis

155 ### 2.3.1 Solids

156 Total suspended solids (TSS) and volatile suspended solids (VSS) were determined according

157 to standard method 2540 (APHA et al., 2012) whereby five replicates of raw wastewater

158 samples (50 mL) were filtered with 1 µm pore size GF/C filters (Whatman). Five blank

159 samples were prepared with 50 mL distilled water.

160 ### 2.3.2 COD, nitrogen and phosphorous

161 Chemical oxygen demand (COD), total nitrogen (total-N), ammonium, nitrate, total

162 phosphorous (total-P) and phosphate were determined using range appropriate commercially

163 available spectrophotometric kits (Spectroquant, Merck). Samples were analysed in

164 triplicates. COD, total-N, and total-P was determined in all wastewater fractions, while

165 ammonium, nitrate, and phosphate were only measured in the TSS-filtrate and in the final

166 permeate.

167 ### 2.3.3 Carbohydrate

168 Carbohydrate concentration was analysed using the anthrone-sulfuric assay with

169 recommended modifications (Leyva et al., 2008). Anthrone reagent (Sigma-Aldrich) was

170 prepared at 0.2 % concentration in concentrated sulphuric acid (Merck Millipore). A dilution

171 series of sucrose (5-1500 mg L^{-1}, VWR) was used as calibration standards. Samples (50 µL)

172 were loaded onto transparent flat-bottom 96-well microtiter plates in quadruplicates before

173 adding 200 µL Anthrone-sulphuric reagent. The contents in the loaded plate were mixed in an

174 ultrasonic bath (10 min), followed by incubation at 95 °C (5 min) and cooling to room

175 temperature. Absorbance was read at 485 nm ± 10 nm with a Tecan Infinite f200 PRO plate

176 reader. Carbohydrate concentrations were transformed to COD equivalents based on an

177   assumed typical composition of $C_{10}H_{18}O_9$ giving 1.12 g COD g^{-1} carbohydrate (Henze et al.,

178   2002).

179   2.3.4   Proteinaceous material

180   Total protein, in this work referred to as proteinaceous material, was determined with the

181   NanoOrange Protein Quantitation Kit (Invitrogen N6666). A calibration standard dilution

182   series was prepared using bovine serum albumin (>98 % heat shock fraction, Sigma-Aldrich)

183   in Milli-Q water. The entire assay and preparative steps was performed in a darkroom with

184   deep red illumination. Wastewater samples (10 % of total reagent volume) and reagent diluent

185   were prepared and loaded onto transparent flat bottom 96-well microtiter plates in

186   quadruplicates. Fluorometry was performed with a Tecan Infinite f200 PRO plate reader at

187   excitation wavelength of 465 nm ± 20 nm and emission wavelength of 590 nm ± 10 nm.

188   Concentrations were transformed to COD equivalents based on a typical average composition

189   of proteinaceous material, $C_{14}H_{12}O_7N_2$, giving 1.20 g COD g^{-1} proteinaceous material (Henze

190   et al., 2002).

191   2.3.5   Lipids

192   Lipid content was determined according to a procedure described in detail in the

193   supplementary information. Total oils and fats were extracted in a 1:1 mixture of chloroform

194   and methanol, and determined gravimetrically. Total lipids and fatty acids composition was

195   determined by GC-FID (Agilent Technologies) following transesterification and methylation

196   of lipids into fatty acid methyl esters (FAME) according to Ryckebosch et al. (2012). Total

197   lipids and free fatty acids concentrations were transformed to COD equivalents based on a

198   typical ThOD of 2.8 g COD g^{-1} lipid, for remaining total oils and fats a reported average of

199   2.03 g COD g^{-1} oils and fats was used (Henze et al., 2002).

2.4   Biodegradability

Biological oxygen demand (BOD) was measured by static respirometry (OxiTop®-C, WTW,

Germany). Test samples were diluted to 200 mg COD L^{-1} final concentration for Vik

wastewater, and to 100 mg COD L^{-1} for Mekjarvik wastewater. Some fractions had lower

COD concentration than 100 mg COD L^{-1}, and for these fractions the highest achievable

concentration based on the concentration after fractionation and upconcentration was used.

Inorganic nutrients, amino acids and vitamins were added as described earlier (Bagi et al.,

2014) and pH was adjusted to ~7. Three replicate test flasks were prepared for each fraction,

and each flask was spiked with sludge: (1) fresh sludge (250 µL) from Vik WWTP for Vik

wastewater fractions, (2) sludge (250 µL) from a fed-batch reactor (initially seeded by the

same Vik sludge) maintained in our laboratory for Mekjarvik wastewater fractions. Test

blanks were prepared by treating autoclaved tap water the same way as wastewater samples.

Oxygen consumption was monitored for 7, 14 or 21 days at 20 °C incubation temperature

under continuous mixing. Oxygen utilisation rate (OUR) was calculated as rate of change in

BOD over six measurement points (gliding average). Both BOD and OUR data were

normalized against initial COD concentration in the test bottles. Biodegradable and inert COD

content in wastewater were estimated as described in supplementary information based on the

method proposed by (Roeleveld and Van Loosdrecht, 2002).

3   Results and discussion

3.1   Wastewater composition

Wastewater composition (COD, Total-N, Total-P, carbohydrate, proteinaceous material, total

oils and fats, total lipids and free fatty acids, biodegradable COD (BCOD) and inert COD) are

summarised in table 1 and 2 for Vik and Mekjarvik wastewater, respectively. Overall

recovery of COD was 78 ± 3 % for Vik wastewater, and 98 ± 4 % for Mekjarvik wastewater

fractionations, respectively. Unidentified COD was determined as the difference between the

225 measured total COD and the sum of identified COD fractions. As expected from upstream

226 sources, a higher total COD (1421 ± 58 mg COD L^{-1}) was measured in raw Vik wastewater,

227 compared to Mekjarvik (690 ± 30 mg COD L^{-1}). Carbohydrate content as a percentage of total

228 COD of 11.6 ± 0.8 % and 57 ± 3 % was found for Vik and Mekjarvik wastewater,

229 respectively. Compared to measured carbohydrate content in raw municipal wastewater from

230 earlier studies (15-36 %; Gorini et al., 2011; Huang et al., 2010; Raunkjær et al., 1994), Vik

231 wastewater had a low carbohydrate content, while Mekjarvik wastewater contained

232 substantially more. The total oils and fats content was 27 ± 2 % and 30 ± 2 %, with a total

233 lipids and free fatty acids content of 21.8 ± 0.9 % and 15.4 ± 0.7 % in Vik and Mekjarvik

234 wastewater, respectively. Lipid content were comparable to literature values (1-38 %; Gorini

235 et al., 2011; Huang et al., 2010; Raunkjær et al., 1994), and represented 51 to 81 % of the total

236 oils and fats. A low content of proteinaceous material was found in both Vik (0.89 ± 0.06 %

237 of total COD) and Mekjarvik wastewater (5.8 ± 0.3 % of total COD) compared to literature

238 values of 16-28 % (Gorini et al., 2011; Huang et al., 2010; Raunkjær et al., 1994). Vik

239 wastewater has a high lipid concentration (table 1) which is known to interfere with the

240 NanoOrange Protein assay (Jones et al., 2003), hence, it is not unlikely that protein content

241 was underestimated. An underestimation of protein content could also explain the high

242 amount of unidentified COD in Vik wastewater (61 ± 5 %).

243 Particle size distribution has in earlier studies been found to directly affect wastewater

244 biodegradability (Dulekgurgen et al., 2006). The size distribution of COD, Total-N, Total-P,

245 macromolecules, BCOD and inert COD among particulate (> 0.65 µm), colloidal (1000 kDa –

246 0.65 µm), polymeric (1-1000 kDa), and oligomeric and monomeric (< 1 kDa) size fractions is

247 presented in figure 1. Relative abundance in each fraction is presented as a percentage

248 (fraction %) of raw wastewater concentrations, except for size fractions with over 100 %

249 recovery (table 1 and table 2). There, the sum of recovered material was used as 100 %

250   instead of the raw wastewater concentration in order to allow for relative comparisons. The

251   majority of COD in Vik wastewater was found in the particulate (36 ± 2 %), and oligomeric

252   and monomeric fractions (40 ± 2 %). In addition, 22 ± 2 % of total COD was unaccounted for

253   during fractionation. Similarly, particulate (44 ± 2 %), and oligomeric and monomeric (53 ± 2

254   %) COD dominated in Mekjarvik wastewater. Low COD concentrations found in polymeric

255   and colloidal size fractions, between 1 kDa and 0.65 µm, corresponds well with the low COD

256   concentrations measured in polymeric size range of municipal wastewater in earlier studies

257   (Doğruel, 2012; Dulekgurgen et al., 2006). Low COD within colloidal and polymeric ranges

258   can be either due to degradation in the sewer system upstream of the WWTP, coagulation and

259   flocculation of polymers and colloids, or degradation of colloids and polymers during the

260   filtration process due to shear stress and enzymatic degradation. Degradation upstream of the

261   WWTP would lead to: (1) an increase of bacterial biomass, which would subsequently appear

262   as high COD in the 0.65-25 µm fraction, and (2) an increase of oligomeric and monomeric

263   partly recalcitrant degradation products, which would appear as high inert COD in the < 1

264   kDa fraction. In addition, if the system has a low active biomass concentration or the biomass

265   is predominantly flocculated or in a biofilm, depolymerisation of colloidal and polymeric

266   COD would lead to increased concentrations of biodegradable COD in the oligomeric and

267   monomeric size fraction (Ravndal and Kommedal, 2017). In our study, both wastewaters had

268   high COD concentrations in these two fractions, and high concentration of inert material was

269   found in the oligomeric and monomeric size fraction (table 1 and table 2). This suggests that

270   significant degradation of COD in the wastewater occurred upstream of the WWTP, and that

271   sewer system hydraulic retention may shift COD size distributions. The latter has been

272   observed by several authors (Hvitved-Jacobsen et al., 2002).

273   The distribution of inert material between size fractions varied between the two studied

274   wastewaters (table 1 and 2). Inert material was estimated by modelling the BOD data using

first order kinetics (supplementary information). Modelling BOD curves using first order

kinetics generally has its limitations due to the models inability to follow complex

degradation patterns. Especially for large particulate fractions with slower initial degradation

and a distinct bimodal growth phase, the first order model gave a poor fit (supplementary

information figure E1). However, for most fractions the first order model reached a

representable ultimate BOD level, thus, a representable inert fraction could be estimated. Vik

wastewater had a higher inert content in the particulate fractions (18 ± 1 %) than Mekjarvik

wastewater (9 ± 1 %). Mekjarvik wastewater was highly dominated by oligomeric and

monomeric inert matter (90 ± 3 %). In Vik wastewater only 32 ± 2 % of inert matter was in

this fraction, however a large fraction of the inerts were not recovered. Compared to Vik

WWTP, Mekjarvik WWTP has a larger inflow of petroleum industry wastewater and urban

runoff. These sources contain a higher fraction of slowly biodegradable priority organic

pollutants and inert pollutants (Kommedal et al., 2016). In addition, high concentrations of

recalcitrant matter in the oligomeric and monomeric size fraction could be a result of

degradation of OM upstream of the WWTP. Mekjarvik WWTP has a longer sewer system

retention time compared to Vik WWTP, allowing for a more complete biodegradation.

Finally, concentrations of inert and unknown COD in the oligomeric and monomeric fraction

in Mekjarvik wastewater are comparable (table 2), further supporting the hypothesis that inert

matter are due to the combination of degradation upstream of the WWTP, and urban runoff

and inflow from the petroleum industry.

Both COD/TN-ratio and COD/TP-ratio decreased with decreasing size fraction for particulate

and colloidal size fractions (figure 2) confirming an earlier study by van Nieuwenhuijzen et

al. (2004). Hence, nitrogen and phosphorous containing substances (e.g. proteinaceous

material and phospholipids) were expected to be more abundant in lower size fractions in

wastewater, while macromolecules not containing nitrogen or phosphorous (e.g. cellulose,

300   starch and lignin) were expected to be more abundant in the large particulate fractions. This

301   corresponds with the analysis of carbohydrates, proteinaceous material and lipids in the two

302   wastewaters. Carbohydrates were abundant in the largest particulate fractions (figure 4),

303   expected due to toilet paper residues (Ruiken et al., 2013). Proteinaceous material content was

304   found to increase with decreasing size for particulate and colloidal size fractions (figure 4),

305   and there was a significant correlation between nitrogen content and content of proteinaceous

306   material (p-value < 0.05, SI). Total lipids and free fatty acids content increase with decreasing

307   size in the particulate fractions (figure 4) and were positively correlated with total-P content

308   in both wastewaters (p-value < 0.05, SI), supporting the theory of phospholipids affecting the

309   trend seen for COD/TP-ratio.

310   3.2   Factors affecting biodegradation of OM in different size fractions

311   Maximum OUR (figure 3) and estimated first order rate constants (k_1, supplementary

312   information table D1) increased with decreasing particle size for both Vik and Mekjarvik

313   wastewater, for the latter the increase continued also with decreasing size for colloids. This

314   confirms earlier results were degradation rate increased with decreasing particle size for

315   faecal particles (Ravndal et al., 2015), egg white particles (Dimock and Morgenroth, 2006)

316   and casein particles (Aldin et al., 2011). Increasing degradation rate with decreasing size can

317   be explained by the particle breakup model proposed by (Dimock and Morgenroth, 2006).

318   Surface area to volume ratio of particles increases with decreasing size, hence substrate

319   availability will increase with decreasing size leading to a faster degradation for smaller

320   particles. In addition, the time it took to reach maximum substrate specific OUR, was

321   significantly higher for the two largest particle fractions of both wastewaters in comparison

322   with the smaller size fractions (figure 3), further supporting a slower degradation of large

323   particulate fractions.

324   Besides OUR and k_1, extent of degradation increased with decreasing particle size

325   (supplementary information, figure D1). A similar increase was also observed for colloids.

326   Extent of degradation should be the same between fractions if chemical composition was the

327   same, hence, we interpret that as being due to a difference in chemical composition between

328   the size fractions (table 1 and table 2). Size dependency on extent of degradation was not

329   observed in earlier studies where extent of biodegradation was independent of particle size

330   (Aldin et al., 2011; Ravndal et al., 2015).

331   Polymeric fractions on the other hand, do not show the same size dependency (figure 3). In

332   fact, Vik wastewater polymeric fractions show the opposite trend with decreasing rate with

333   decreasing size, however, no trend was observed for Mekjarvik wastewater. For polymers

334   with identical chemical composition, such as dextran standards, degradation rate increase with

335   decreasing size (Kommedal et al., 2006). The polymeric wastewater fractions differed in

336   chemical composition (table 1 and table 2), and we suggest differences in chemical

337   composition to be more important for biodegradation rate than differences in polymer size in

338   the polymeric fractions.

339   3.3   Analytical validation of size fractionation

340   In earlier studies, validation of size fractionation has not been performed (Dulekgurgen et al.,

341   2006; Karahan et al., 2008; Sophonsiri and Morgenroth, 2004). When serial filtering

342   wastewater, actual size distribution of OM in the different size fractions can differ from the

343   nominal membrane cut-off due to filter cake retention, induced shear stress, shape of

344   molecules, concentration polarization and membrane rejection (Logan and Jiang, 1990).

345   These effects result in an underestimation of low molecular weight compounds. On the

346   contrary, induced shear stress may degrade particulate and large polymeric materials,

347   increasing the lower molecular weight fractions. In earlier studies, such as the studies by

348   Dulekgurgen et al. (2006) and Huang et al. (2010) this was not considered. Sophonsiri and

349 Morgenroth (2004) used parallel filtration when possible to overcome these problems,

350 however, filter clogging led to the need to serially filter some samples. To minimise cake

351 formation and concentration polarisation, and to control the mass balance and estimate

352 recovery, serial filtration using tangential flow filtration was selected in this study.

353 Particle size distribution (PSD), rms radius, and molecular weight distributions for Mekjarvik

354 wastewater are presented in figure 5. Based on PSD data, the 100-1000 µm fraction contained

355 a significant amount of particles smaller than nominal sieve cut-off (approximately 70 % of

356 particle volume). The same was observed in the 25-100 µm fractions, but to a lesser extent

357 (36 %). Retention of particles smaller than nominal sieve cut-off probably occurred due to

358 filter cake retention. Observed PSD in the 0.65-25 µm fraction seem to fall well within the

359 defined limits for the macroscopic particles (> 2 µm). However, we observed severe

360 membrane fouling of the 0.65 µm membrane which most likely led to increased retention of

361 colloids and polymers below the 0.65 µm nominal cut-off. Evidently, the fractions

362 immediately below 0.65 µm had much lower COD concentrations (table 1 and 2). In spite of

363 this, chemical composition and biodegradability of the immediately lower size fractions are

364 expected to be representative due to non-selective retention. Cumulative weight average

365 molecular weight and particle diameter of colloidal and polymeric size fractions (figure 5)

366 show a decrease in diameter or molecular weight with descending nominal filter cut-off,

367 however, molecules and particles larger than membrane cut-off was present. For polymeric

368 fractions, a larger shift towards higher size fractions was seen for size fractions with

369 decreasing molecular weight. This could be an effect of the shape of the molecules, or

370 alternatively, a result of overrepresentation of larger molecules in the MALS technique, since

371 bigger molecules scatter light exponentially more than small ones (Wyatt, 1993).

3.4 Implications for wastewater treatment processes and resource recovery

Detailed analysis of wastewater composition is a prerequisite for potential resource recovery from wastewater. Size distributions are important for development and selection of adequate unit processes, and both elemental and macromolecular information are necessary for proper recovery estimations with respect to the aforementioned unit processes. In addition, both design and operation of novel and complex recovery plants would benefit greatly from the use of advanced bioprocess models able to predict and systematically analyse system performance. Compared to the existing modelling frameworks used in the field (ASM and ADM models), this would probably mean higher model resolution (several fractional state variables), and several stoichiometric and kinetic parameters. Consequently, compositional analysis as presented in this work is required, both in terms of size fractionation and chemical species composition. By combining particle size distribution, chemical composition, and biodegradability analysis, an example of such an analysis is given of two wastewaters representing two very different scenarios for recovery: The classical household and diverse industrial and the food-industrial dominated municipal wastewaters. In both wastewaters, the two largest particulate fractions (> 1 mm and 100 µm – 1 mm) contained mainly carbohydrates (table 1 and table 2), likely due to toilet paper residuals. Earlier research has shown that sieving raw wastewater with 0.35 mm has great potential to recover slowly biodegradable cellulose from toilet paper, recovered cellulose could be used as feedstock for biofuel production or for production of new toilet paper (Ruiken et al., 2013). Based on the results of this study sieves down to 0.1 mm might be applicable for extraction of cellulose from raw wastewater. Removing the large particulate fraction mainly composed of slowly degradable carbohydrates early, could lead to more efficient biological treatment stages downstream of the sieves.

17

The particulate size fractions between 0.65-100 µm has a high lipids content in both

wastewaters. The reason for this is unclear, however, in the dairy dominated Vik wastewater

we suspect this to be lipid micelles from milk fat, and presence of general fat globules (both

known to be in the lower µm range; Fox and McSweeney, 2006). The most abundant lipids in

these size fraction were C16 (relative concentration 38 % in Vik wastewater and 31 % in

Mekjarvik wastewater, SI) and C18 lipids (relative concentration 43 % in Vik wastewater and

54 % in Mekjarvik wastewater, SI). In addition, a high saturation levels of C16 and C18 was

found in both wastewaters (combined saturation level of 62 % in Vik wastewater and 58 % in

Mekjarvik wastewater, SI). Abundance of highly saturated C16 and C18 lipids is ideal for

biodiesel production (Zhu et al., 2017), hence, the two size fractions between 0.65-100 µm are

appropriate fractions for direct biofuel recovery.

Enhanced energy recovery by biogas production and treatment process energy efficiency are

both dependent on the ability of wastewater treatment unit processes to separate COD

containing components before bacterial oxidation (Sutton et al., 2011). This is a key argument

used for anaerobic wastewater treatment, however, residual effluent COD and lack of nutrient

removal mechanisms limit its use as stand-alone processes. Another strategy is to maximize

separation of COD containing components from the raw wastewater upstream of

bioconversion processes by enhanced primary treatment (Verstraete et al., 2009). Our results

indicate that the particulate fraction that normally do not settle in the primary settler, the 0.65

– 25 µm fraction contain 15-22 % of the raw COD (almost all biodegradable), would upon

adequate separation significantly enhance energy performance and recovery. Furthermore, the

high lipid content in this fraction would stimulate biogas production potential, as the specific

COD of lipids are high. Contrary to energy, nutrient recovery potential in the particulate

fractions are limited. About 80 % of the size class specific nutrients are found in the low M_W

dissolved fraction (> 1 kDa), and unit operations for direct recovery should focus on these.

421 While this paper focus on wastewater characterization and potential for resource recovery,

422 recovery also rely on the technological and economic feasibility. Ruiken et al. (2013)

423 presented an economic and technical evaluation of cellulose recovery from municipal

424 wastewater, and concluded sieving of the $> 350\,\mu m$ fraction to be a feasible energy recovery

425 and efficiency measure. Lipids recovery, as highlighted here as a potential resource, has been

426 technically and economically evaluated using algal bioreactors, but full-scale implementation

427 is still a challenge due to unfeasible technical or economical limitations (Zhu et al, 2017). Of

428 the several challenges summarized, efficient and economically favourable extraction and

429 purification unit processes needs to be developed for wastewater lipids recovery.

430 ## 4   Conclusions

431 We investigated biodegradability, COD and nutrient composition on detailed size fractionated

432 wastewaters. To our knowledge, this is the most detailed and comprehensive compositional

433 analysis published and allow for novel strategies for modelling and resource recovery. Key

434 findings are:

435 • Particulate size fractions larger than 100 µm are highly abundant in carbohydrates,

436   possibly from toilet paper, that can be recovered by sieving. The particulate size

437   fractions between 0.65-100 µm are highly abundant in highly saturated C16 and C18

438   lipids, making these size fractions a good source for lipids extraction for biodiesel

439   production.

440 • Biodegradation rates of particles in wastewater were controlled by particle size, i.e.,

441   surface area to volume ratio of the organic matter, resulting in smaller particles having

442   higher degradation rates. In the polymeric fraction, degradation rates of soluble

443   polymeric organic matter were governed by chemical composition and not by polymer

444   size.

445   • The two municipal wastewaters analysed here were dominated by particulate and

446   oligomeric and monomeric size organic matter. Very little COD was found in

447   polymeric and colloidal fractions, possibly due to degradation in the sewer upstream

448   from WWTP.

449   • Overall recovery of organic material was relatively high in both fractionation

450   experiments. Analytical validation of actual PSD in our size-fractions showed below

451   filter cut-off retention of particles close to nominal cut-off in particulate size ranges,

452   leading to PSD shifting to lower sizes. An opposite trend was observed for polymeric

453   fractions, where a shift towards higher than the nominal membrane pore sizes was

454   seen.

5   Acknowledgements

6   References

463 Aldin, S., Nakhla, G., Ray, M.B., 2011. Modeling the influence of particulate protein size on

464   hydrolysis in anaerobic digestion. Ind. Eng. Chem. Res. 50, 10843–10849.

465   doi:10.1021/ie200385e

466 APHA, AWA, WEF, 2012. Standard method for examination of water and wastewater, 22nd

467   ed. American Public Health Association, Washington.

468 Asano, T., Levine, A.D., 1998. Wastewater reclamation, recycling and reuse: An introduction,

469   in: Asano, T. (Ed.), Wastewater Reclamation and Reuse: Water Quality Management

470   Library, Volume X. CRC Press, Boca Raton, pp. 1–56.

471 Bagi, A., Pampanin, D.M., Lanzén, A., Bilstad, T., Kommedal, R., 2014. Naphthalene

472   biodegradation in temperate and arctic marine microcosms. Biodegradation 25, 111–125.

473   doi:10.1007/s10532-013-9644-3

474 Cheong, K.-L., Wu, D.-T., Zhao, J., Li, S.-P., 2015. A rapid and accurate method for the

475   quantitative estimation of natural polysaccharides and their fractions using high

476   performance size exclusion chromatography coupled with multi-angle laser light

477   scattering and refractive index detector. J. Chromatogr. A 1400, 98–106.

478   doi:10.1016/j.chroma.2015.04.054

479 Cheryan, M., 1998. Ultrafiltration and microfiltration handbook. CRC Press, Boca Raton,

480   Florida.

481 Choubert, J.M., Rieger, L., Shaw, A., Copp, J., Spérandio, M., Sørensen, K., Rönner-Holm,

482   S., Morgenroth, E., Melcer, H., Gillot, S., 2013. Rethinking wastewater characterisation

483   methods for activated sludge systems - A position paper. Water Sci. Technol. 67, 2363–

484   2373. doi:10.2166/wst.2013.158

485 Dimock, R., Morgenroth, E., 2006. The influence of particle size on microbial hydrolysis of

486   protein particles in activated sludge. Water Res. 40, 2064–2074.

487   doi:10.1016/j.watres.2006.03.011

488 Doğruel, S., 2012. Biodegradation characteristics of high strength municipal wastewater

489   supported by particle size distribution. Desalin. Water Treat. 45, 11–20.

490   doi:10.1080/19443994.2012.691955

491 Dulekgurgen, E., Doğruel, S., Karahan, Ö., Orhon, D., 2006. Size distribution of wastewater

492   COD fractions as an index for biodegradability. Water Res. 40, 273–282.

493   doi:10.1016/j.watres.2005.10.032

494   Fox, P.F., McSweeney, P.L.H., 2006. Advanced Dairy Chemistry: Vol 2 Lipids., 3rd ed.

495   Springer, New York.

496   Gorini, D., Choubert, J.M., Le Pimpec, P., Heduit, A., 2011. Concentrations and fate of

497   sugars, proteins and lipids during domestic and agro-industrial aerobic treatment. Water

498   Sci. Technol. 63, 1669–1677. doi:10.2166/wst.2011.334

499   Harmsen, G.J., 2007. Reactive distillation : The front-runner of industrial process

500   intensification A full review of commercial applications, research, scale-up, design and

501   operation. Chem. Eng. Process. 46, 774–780. doi:10.1016/j.cep.2007.06.005

502   Henze, M., Harremoës, P., la Cour Jansen, J., Arvin, E., 2002. Wastewater treatment.

503   Springer, Berlin.

504   Huang, M., Li, Y., Gu, G., 2010. Chemical composition of organic matters in domestic

505   wastewater. Desalination 262, 36–42. doi:10.1016/j.desal.2010.05.037

506   Hvitved-Jacobsen, T., Vollertsen, J., Matos, J.S., 2002. The sewer as a bioreactor - a dry

507   weather approach. Water Sci. Technol. 45, 11–24.

508   Jones, L.J., Haugland, R.P., Singer, V.L., 2003. Development and characterization of the

509   NanoOrange protein quantitation assay: A fluorescence-based assay of proteins in

510   solution. Biotechniques 34, 850–861.

511   Karahan, Ö., Dogruel, S., Dulekgurgen, E., Orhon, D., 2008. COD fractionation of tannery

512   wastewaters-Particle size distribution, biodegradability and modeling. Water Res. 42,

513   1083–1092. doi:10.1016/j.watres.2007.10.001

514   Kommedal, R., Milferstedt, K., Bakke, R., Morgenroth, E., 2006. Effects of initial molecular

515   weight on removal rate of dextran in biofilms. Water Res. 40, 1795–1804.

516   doi:10.1016/j.watres.2006.02.032

517   Kommedal, R., Ydstebø, L., Bilstad, T., 2016. Occurrence and fate of priority organic

518   pollutants during wastewater sludge treatment, in: 5th International Conference on

519   Industrial and Hazardous Waste Management, 27-30th September 2016, Chania, Crete.

520   Levine, A.D., Tchobanoglous, G., Asano, T., 1991. Size distributions of particulate

521   contaminants in wastewater and their impact on treatability. Water Res. 25, 911–922.

522   doi:10.1016/0043-1354(91)90138-G

523   Leyva, A., Quintana, A., Sánchez, M., Rodríguez, E.N., Cremata, J., Sánchez, J.C., 2008.

524   Rapid and sensitive anthrone-sulfuric acid assay in microplate format to quantify

525   carbohydrate in biopharmaceutical products: Method development and validation.

526   Biologicals 36, 134–141. doi:10.1016/j.biologicals.2007.09.001

527   Logan, B.E., Jiang, Q., 1990. Molecular size distribution of dissolved organic matter. J.

528   Environ. Eng. 116, 1046–1062.

529   Matassa, S., Batstone, D.J., Hülsen, T., Schnoor, J., Verstraete, W., 2015. Can direct

530   conversion of used nitrogen to new feed and protein help feed the world? Environ. Sci.

531   Technol. 49, 5247–5254. doi:10.1021/es505432w

532   Puchongkawarin, C., Gomez-Mont, C., Stuckey, D.C., Chachuat, B., 2015. Chemosphere

533   Optimization-based methodology for the development of wastewater facilities for energy

534   and nutrient recovery. Chemosphere 140, 150–158.

535   doi:10.1016/j.chemosphere.2014.08.061

536   Puyol, D., Batstone, D.J., Hülsen, T., Astals, S., Peces, M., Krömer, J.O., 2017. Resource

537   recovery from wastewater by biological technologies: Opportunities, challenges, and

538   prospects. Front. Microbiol. 7, 1–23. doi:10.3389/fmicb.2016.02106

539   Raunkjær, K., Hvitved-Jacobsen, T., Nielsen, P.H., 1994. Measurement of pools of protein,

540   carbohydrate and lipid in domestic wastewater. Water Res. 28, 251–262.

541   Ravndal, K.T., Kommedal, R., 2017. Starch degradation and intermediate dynamics in

542   flocculated and dispersed microcosms. Water Sci. Technol. In Press.

543   doi:10.2166/wst.2017.467

544 Ravndal, K.T., Künzle, R., Derlon, N., Morgenroth, E., 2015. On-site treatment of used wash-

545   water using biologically activated membrane bioreactors operated at different solids

546   retention times. J. Water Sanit. Hyg. Dev. 4, washdev2015174.

547   doi:10.2166/washdev.2015.174

548 Roeleveld, P.J., Van Loosdrecht, M.C.M., 2002. Experience with guidelines for wastewater

549   characterisation in The Netherlands. Water Sci. Technol. 45, 77–87.

550 Ruiken, C.J., Breuer, G., Klaversma, E., Santiago, T., van Loosdrecht, M.C.M., 2013. Sieving

551   wastewater - Cellulose recovery, economic and energy evaluation. Water Res. 47, 43–48.

552   doi:10.1016/j.watres.2012.08.023

553 Ryckebosch, E., Muylaert, K., Foubert, I., 2012. Optimization of an analytical procedure for

554   extraction of lipids from microalgae. JAOCS, J. Am. Oil Chem. Soc. 89, 189–198.

555   doi:10.1007/s11746-011-1903-z

556 Sophonsiri, C., Morgenroth, E., 2004. Chemical composition associated with different particle

557   size fractions in municipal, industrial, and agricultural wastewaters. Chemosphere 55,

558   691–703. doi:10.1016/j.chemosphere.2003.11.032

559 Sutton, P.M., Melcer, H., Schraa, O.J., Togna, A.P., 2011. Treating municipal wastewater

560   with the goal of resource recovery. Water Sci. Technol. 63, 25–31.

561   doi:10.2166/wst.2011.004

562 Tran, N.H. an, Ngo, H.H. ao, Urase, T., Gin, K.Y. ew H., 2015. A critical review on

563   characterization strategies of organic matter for wastewater and water treatment

564   processes. Bioresour. Technol. 193, 523–533. doi:10.1016/j.biortech.2015.06.091

565 van Loosdrecht, M.C.M., Brdjanovic, D., 2014. Anticipating the next century of wastewater

566   treatment. Science. 344, 1452–1453. doi:10.1126/science.1255183

567 van Nieuwenhuijzen, A.F., van der Graaf, J.H.J.M., Kampschreur, M.J., Mels, A.R., 2004.

568   Particle related fractionation and characterisation of municipal wastewater. Water Sci.

569   Technol. 50, 125–132.

570   Verstraete, W., Van de Caveye, P., Diamantis, V., 2009. Maximum use of resources present

571   in domestic "used water." Bioresour. Technol. 100, 5537–5545.

572   doi:10.1016/j.biortech.2009.05.047

573   Wahlen, B.D., Willis, R.M., Seefeldt, L.C., 2011. Biodiesel production by simultaneous

574   extraction and conversion of total lipids from microalgae, cyanobacteria, and wild

575   mixed-cultures. Bioresour. Technol. 102, 2724–2730.

576   doi:10.1016/j.biortech.2010.11.026

577   Wang, X., McCarty, P.L., Liu, J., Ren, N.-Q., Lee, D.-J., Yu, H.-Q., Qian, Y., Qu, J., 2015.

578   Probabilistic evaluation of integrating resource recovery into wastewater treatment to

579   improve environmental sustainability. Proc. Natl. Acad. Sci. 112, 1630–1635.

580   doi:10.1073/pnas.1410715112

581   Wilsenach, J.A., Maurer, M., Larsen, T.A., van Loosdrecht, M.C., 2003. From waste

582   treatment to integrated resource management. Water Sci. Technol. 48, 1–9.

583   Wyatt, P.J., 1993. Light scattering and the absolute characterization of macromolecules. Anal.

584   Chim. Acta 272, 1–40.

585   Wyatt Technology (2017) https://www.wyatt.com/solutions/techniques/sec-mals-molar-mass-

586   size-multi-angle-light-scattering.html accessed on 12 December, 2017.

587   Zhao, H., Brown, P.H., Schuck, P., 2011. On the distribution of protein refractive index

588   increments. Biophys. J. 100, 2309–2317. doi:10.1016/j.bpj.2011.03.004

589   Zhu, F., Wu, X., Zhao, L., Liu, X., Qi, J., Wang, X., Wang, J., 2017. Lipid profiling in sewage

590   sludge 116. doi:10.1016/j.watres.2017.03.032

591   Zhu L. Nugroho Y.K., Shakeel S.R., Li Z., Martinkauppi B. and Hiltunen E. (2017) Using

592   microalgae to produce liquid transportation biodiesel: What is next? Renewable and

593   Sustainable Energy Reviews, 78, 391-400. doi: 10.1016/j.rser.2017.04.089

Table 1: Concentration of COD, total-N, total-P, carbohydrate, proteinaceous material, total oils and fats, and total lipids and free fatty acids in raw wastewater (WW), TSS filtrate and all size fractions from Vik wastewater (± standard error)

| Fraction	COD (mg L^{-1})	Total-N (mg N L^{-1})	Total-P (mg P L^{-1})	Carbohydrate (mg COD L^{-1})	Proteinaceous material (mg COD L^{-1})	Oils and fats (mg COD L^{-1})	Lipids and free fatty acids (mg COD L^{-1})	Unidentified (mg COD L^{-1})	Inert (mg COD L^{-1})	Biodegradable (mg COD L^{-1})
Raw WW	1421 ± 58	62 ± 6	10.7 ± 0.6	165 ±.8	12.6 ± 0.6	382 ± 16	310 ± 1	862 ± 61	506 ± 21	915 ± 38
TSS filtrate	590 ± 7	43 ± 1	6.62 ± 0.04	n/a	n/a	n/a	n/a	n/a	n/a	n/a
> 1 mm	113 ± 4	1.13 ± 0.05	0.30 ± 0.07	109 ± 45	0.72 ± 0.04	18.4 ± 0.6	14.74 ± 0.04	0	17 ± 1	97 ± 7
100 µm – 1 mm	51 ± 4	0.82 ± 0.05	0.19 ± 0.01	39 ± 18	1.4 ± 0.5	8.9 ± 0.4	5.69 ± 0.06	1 ± 18	15 ± 2	36 ± 4
25 – 100 µm	32.2 ± 0.6	0.76 ± 0.02	0.144 ± 0.003	5.9 ± 0.4	0.9 ± 0.2	15.1 ± 0.5	10.3 ± 0.5	10 ± 1	7.6 ± 0.5	25 ± 2
0.65 – 25 µm	318 ± 2	5.4 ± 0.4	1.03 ± 0.05	16 ± 2	9.7 ± 0.4	225 ± 3	200 ± 1	67 ± 5	54 ± 4	263 ± 17
0.1 – 0.65 µm	3.14 ± 0.08	0.150 ± 0.002	0.025 ± 0.002	0.41 ± 0.05	< 0.04	n/a	n/a	2.7 ± 0.1	1.66 ± 0.06	1.49 ± 0.05
1000 kDa – 0.1 µm	0.38 ± 0.04	0.016 ± 0.002	0.0039 ± 0.0004	< 0.15	< 0.04	1.4 ± 0.1	1.2 ± 0.9	0	0.20 ± 0.02	0.18 ± 0.02
100 – 1000 kDa	0.83 ± 0.02	0.050 ± 0.002	0.0082 ± 0.0003	0.23 ± 0.03	< 0.04	1.6 ± 0.1	1 ± 1	0	0.29 ± 0.03	0.54 ± 0.06
10 – 100 kDa	4.30 ± 0.02	0.317 ± 0.02	0.040 ± 0.002	0.9 ± 0.1	0.26 ± 0.02	3.6 ± 0.2	1 ± 1	0	0.54 ± 0.04	3.8 ± 0.3
1 – 10 kDa	16.4 ± 0.1	1.07 ± 0.02	0.093 ± 0.002	5.2 ± 0.6	0.63 ± 0.08	6.2 ± 0.2	0.152 ± 0.002	4.4 ± 0.7	0.5 ± 0.3	16 ± 12
< 1 kDa	567 ± 5	36.3 ± 1	6.5 ± 0.2	66 ± 8	1.72 ± 0.08	149 ± 9	0.00 ± 0.00	351 ± 13	161 ± 5	406 ± 13
Recovery (%)	78 ± 3	74 ± 8	78 ± 5	147 ± 30	122 ± 8	112 ± 5	75.7 ± 0.8	50 ± 4	51 ± 2	93 ± 5

1 **Table 2:** Concentration of COD, total-N, total-P, carbohydrate, proteinaceous material, total oils and fats, and total lipids and free fatty acids in raw wastewater (WW),

2 TSS filtrate and all size fractions from Mekjarvik wastewater (± standard error)

Fraction	COD (mg L^{-1})	Total-N (mg N L^{-1})	Total-P (mg P L^{-1})	Carbohydrate (mg COD L^{-1})	Proteinaceous material (mg COD L^{-1})	Oils and fats (mg COD L^{-1})	Lipids and free fatty acids (mg COD L^{-1})	Unidentified (mg COD L^{-1})	Inert (mg COD L^{-1})	Biodegradable (mg COD L^{-1})
Raw WW	690 ± 30	37 ± 1	5.0 ± 0.2	395 ± 16	39.9 ± 0.8	209 ± 12	106 ± 2	47 ± 36	191 ± 10	499 ± 27
TSS filtrate	262 ± 10	27 ± 1	2.6 ± 0.2	n/a	n/a	n/a	n/a	n/a	121 ± 6	142 ± 7
> 1 mm	139 ± 5	0.53 ± 0.02	0.286 ± 0.003	149 ± 23	1.09 ± 0.02	37.3 ± 0.6	21.4 ± 0.1	0	11 ± 3	128 ± 37
100 µm – 1 mm	27 ± 4	0.37 ± 0.02	0.053 ± 0.002	45 ± 5	0.31 ± 0.04	5.5 ± 0.2	4.5 ± 0.5	0	5.6 ± 0.8	22 ± 3
25 – 100 µm	37.2 ± 0.8	1.07 ± 0.03	0.184 ± 0.004	11.1 ± 0.3	1.04 ± 0.05	17.9 ± 0.5	11.7 ± 0.1	7 ± 1	5.3 ± 0.5	32 ± 3
0.65 – 25 µm	101.6 ± 0.9	3.4 ± 0.2	0.71 ± 0.03	15.4 ± 0.3	1.9 ± 0.1	45.4 ± 0.4	30.9 ± 0.4	39 ± 1	2.5 ± 0.5	99 ± 18
0.1 – 0.65 µm	0.64 ± 0.02	0.0412 ± 0.0005	0.0053 ± 0.0007	0.47 ± 0.01	0.022 ± 0.002	0.00 ± 0.00	0.044 ± 0.001	0.13 ± 0.03	0.06 ± 0.04	0.6 ± 0.4
1000 kDa – 0.1 µm	0.20 ± 0.02	0.0264 ± 0.0005	0.0035 ± 0.0007	0.54 ± 0.03	0.023 ± 0.002	0.00 ± 0.00	0.08 ± 0.04	0	0.035 ± 0.003	0.17 ± 0.02
100 – 1000 kDa	0.382 ± 0.009	0.0345 ± 0.0004	0.0036 ± 0.0006	0.52 ± 0.03	0.026 ± 0.002	0.00 ± 0.00	0.04 ± 0.07	0	0	0.382 ± 0.009
10 – 100 kDa	2.6 ± 0.3	0.0065 ± 0.0006	0.0071 ± 0.0009	1.36 ± 0.05	0.080 ± 0.003	0.00 ± 0.00	0.021 ± 0.002	1.2 ± 0.3	0.71 ± 0.09	1.9 ± 0.3
1 – 10 kDa	6.36 ± 0.06	0.244 ± 0.009	0.024 ± 0.001	1.7 ± 0.2	0.42 ± 0.01	6.4 ± 0.2	0.299 ± 0.001	0	1.2 ± 0.2	5.2 ± 0.8
< 1 kDa	363 ± 5	25 ± 1	2.9 ± 0.2	108 ± 2	5.9 ± 0.4	25 ± 3	7.68 ± 0.09	224 ± 6	233 ± 6	131 ± 3
Recovery (%)	98 ± 4	83 ± 4	83 ± 4	84 ± 7	27 ± 1	66 ± 4	72 ± 2	580 ± 448	136 ± 8	84 ± 9

3

1
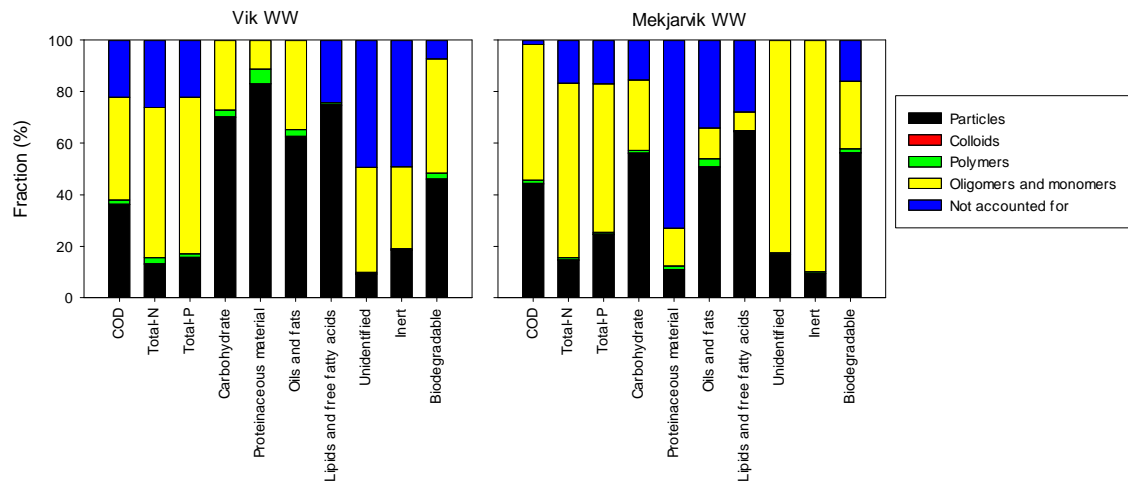
Figure 1: Size distribution of OM in particulate (>0.65 µm), colloidal (1000 kDa – 0.65 µm), polymeric (1-1000

kDa) and truly dissolved (< 1 kDa) size ranges. Calculations are based on raw wastewater measurement except

for carbohydrate, proteinaceous material, and oils and fats for Vik wastewater, and unidentified and inert

material for Mekjarvik wastewater, where the sum of material in the size fractions is used due to a recovery

higher than 100 %

7
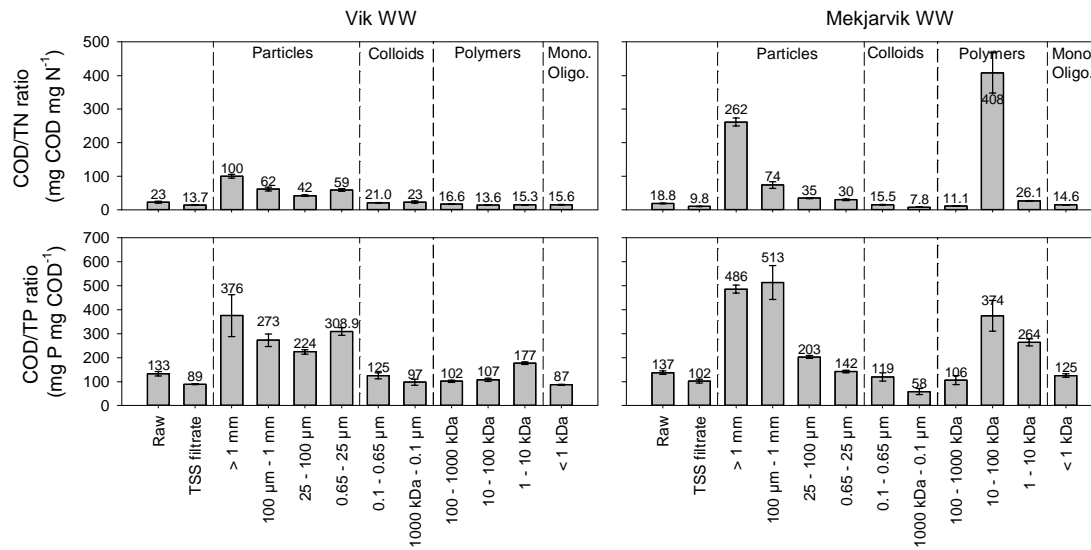
1

2 **Figure 2:** COD/TN and COD/TP in raw wastewater and all size fractions for Vik and Mekjarvik wastewater.

3 Error bars show standard deviations calculated for relative values.

1
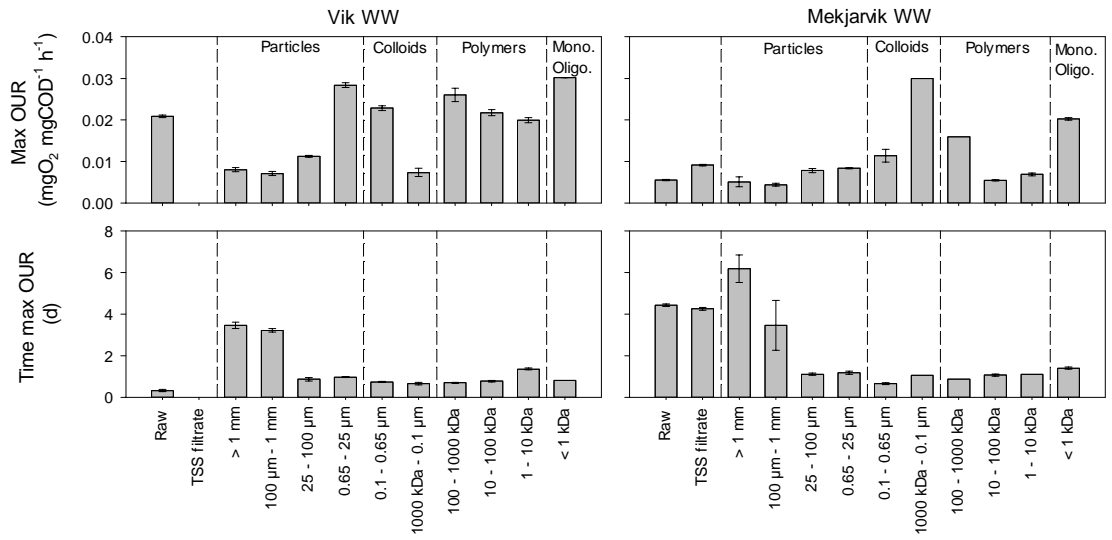
Figure 3: Max OUR (mg O_2 mg COD^{-1} h^{-1}) and time to reach max OUR (d). Error bars show standard error. *)

1000 kDa – 0.1 µm and 100-1000 kDa fraction Mekjarvik wastewater data from only one parallel, the rest

average of data from three parallels.

5

1
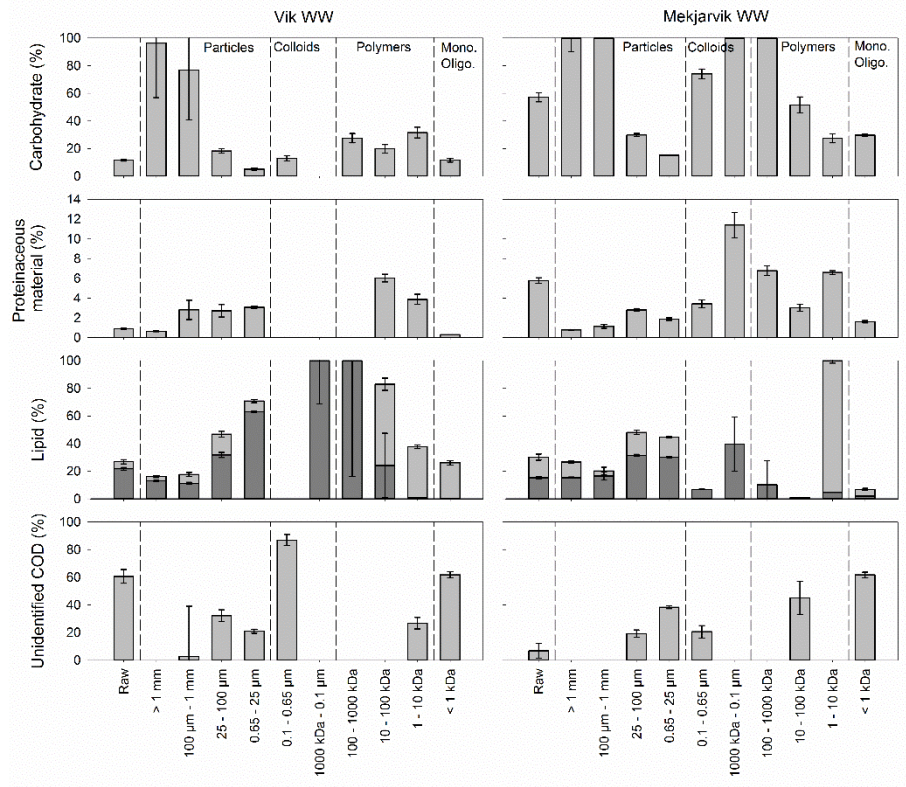
Figure 4: Content of carbohydrate, proteinaceous material, lipids as total oils and fats (light grey) and total lipids

and fatty acids (dark grey), and unidentified COD in raw wastewater and all size fractions for Vik and Mekjarvik

wastewater. Percentage was calculated as percentage of measured COD in each individual fraction. Error bars

show standard deviations calculated for relative values.
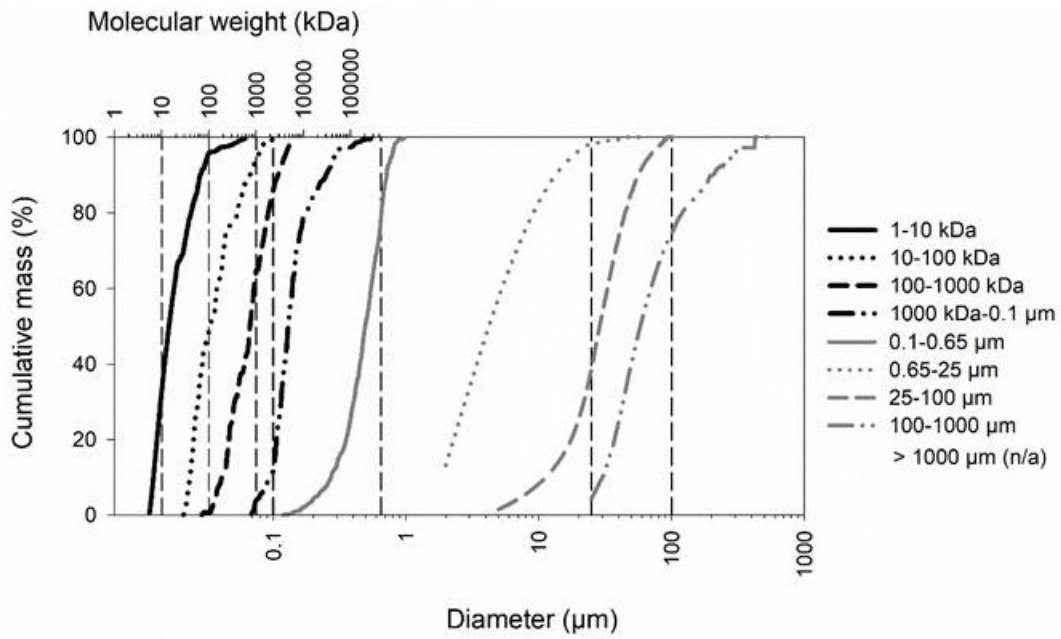
Figure 5: Analysed size distribution in size fractionated wastewater from Mekjarvik WWTP. Particulate fractions are based on volume measurements and density was assumed constant between fractions.

Supplementary information

A. Serial filtration of wastewater

Figure A1 shows the WW-fractionation setup, the left section shows the initial sieving while the right section shows the tangential flow filtration (TFF) stages. During the sieving process, raw wastewater was fed with a peristaltic pump onto a column holding the three sieves with consecutively smaller cut-offs. A small amount of washing water (Milli-Q pH 2.3 adjusted with HCl) was used to remove trapped sub-fraction particles. The amount of washing water was recorded and the water itself was pooled together with the rest of filtered WW. The sieving-filtrate was then transferred to the TFF feed tank (first pass). During the TFF, the system was run in a continuously fed batch mode until all the water had passed through each filter. The first TFF run was carried out with the 0.65 µm cutoff filter. At the end of the run, a small amount of washing water was added to the concentrate to wash out salts and trapped sub-fraction particles. Again, the amount of the washing water was measured and the water itself was pooled together with the filtrate. This washing step was carried out at each filtration stage. The fraction concentrate was drained from the lowest point of the TFF system unassisted until it stopped flowing. Finally, the filtrate was returned to the clean and emptied TFF feed tank and the process was repeated using the next filter (0.1 µm cutoff). Similarly, four more rounds were carried out with to complete the size fractionation. Throughout the entire TFF process, temperatures were logged externally for the concentrate tank, feed tank, membrane filter and filtrate tanks. Feed, transmembrane and delta pressures were also logged in order to keep track of filter performance. The weight of concentrate was set as a trigger to stop the process preventing running the system dry. In addition, coolant loops and heat

exchangers where either submerged in tanks or placed in line to keep the wastewater

cool. The WW were also continuously mixed at 200 rpm or circulated to prevent settling.

Figure A1: Experimental setup of the serial filtration process. The wastewater was first sieved, followed by micro and ultrafiltration with a tangential flow filtration setup.

B. Determination of lipids content in wastewater

Total oils and fats extraction

All glassware and volumetric equipment were rinsed using a 1:1 mixture of analytical

grade Methanol (NOMAPURE, VWR Int.) and Chloroform (EMSURE, Merck GmbH).

Volumetric aliquots (about 10 ml) of concentrated fractionated wastewater was

quantitatively transferred to Teflon sealed 200 ml Schott bottles (Duran Group GmBH)

and mixed with 20 ml Chloroform and 20 ml Methanol. Lipids were extracted for a

minimum of 2 hours on a shaker, intermittently sonicated for 2x8 min on a Branson 2510

sonicator at 50°C/100 W (Branson Ultrasonics, Danbury CT, USA). Following

extraction, the mixture was quantitatively transferred to a 250 ml separation funnel and

left overnight for phase separation. The lower fraction was collected, and the liquid re-

extracted two times by shaking using 20 ml Chloroform and 10 ml deionized water. The

combined extract was transferred to a Syncore analyst (BÜCHI Labortechnik AG, CH), vacuum distiller and concentrated to < 1 ml (at 55°C and 250 mbar A). The concentrate was quantitatively transferred to a Teflon lined 10 ml vial using an additional 3-4 ml Chloroform and stored in the dark at 4°C.

Clean up

Extracted samples were transferred to 15 ml conical Duran glass centrifuge tubes and added 1 ml distilled water, vortexed and centrifuged at 1000 g for 5 min. The upper layer was removed using a Pasteur pipette, while the lower Chloroform layer was transferred to an anhydrous Na_2SO_4 packed glass column for residual water removal. The removed water layer was transferred back to the centrifuge tube, and re-extracted using 5 ml of 1:1 Chloroform-Methanol and dried over the same column (same procedure as above). The combined extracts were evaporated to dryness by a gentle stream of Argon inside a 50°C heat block, and resuspended in 2 ml Toluene:Methanol (2:1). 1 ml was transferred to a 2 ml glass vial for gravimetric determination of total oil and fats, while the remaining sample (1.00 ml) was used for total lipids determination.

Gravimetric determination of total oils and fats

The 1.00 ml oil and fats extract was evaporated to dryness in a Visiprep SPE Vacuum manifold (Supelco Inc) to dryness by a gentle stream of Argon at 250 mbar A. Following vacuum drying, the sample was weighed using a high precision analytical balance (0.01 mg resolution, Mettler Toledo model XSE). The vial was dried for another 15 min until constant weight. Total oils and fats was removed using repeated flushing using a 1:1 Chloroform – Methanol mixture, and the vials were vacuum dried until constant weight.

Total oils and fats was determined as the differential weight before and after oil and fats removal.

Derivatisation and analysis of total lipids

Total lipids and fatty acids composition was determined by GC-FID following transesterification and methylation of lipids into fatty acid methyl esters (FAME) according to Ryckebosch et al. (2012). 1 ml of fresh 2% (v/v) sulfuric acid (pro analysis, VWR Int.) in methanol (NOMAPURE, VWR Int.) was added to the remaining 1.00 ml total oils and fats extract (above). The sample was vortexed and left for lipids methylation for 1 hour at 80°C. After methylation and cooling to room temperature, 0.5 ml 5 M aqueous NaCl solution was added and sample vortexed, followed by addition of 2 ml Hexane (HiPerSolv CHROMANORM® for HPLC, VWR chemicals) and vortexing. The samples were centrifuged for 2 min at 1000 g, and the upper layer transferred to a glass column packed with anhydrous Na_2SO_4 for drying. Samples were re-extracted by another 2 ml Hexane and 1 ml water, centrifuged and the hexane layer dried and combined with the initial upper layer. The methylated extract was dried under a gentle stream of Argon at 50°C (in heat block), and upon drying, resuspended in 1000 µl Hexane:Chloroform (2:1) mixture for GC analysis.

FAME distribution and quantification was determined using an Agilent 6890 gas chromatograph equipped with an Agilent J&W DB-225MS capillary column (PN 122-2932) operated in constant pressure mode, using Helium as carrier gas. 1 µl sample was injected using a Gerstel MPS liquid mode sampler onto a 220°C pulsed split inlet (50:1 split ratio, at 350 kPa for initial 0.5 min, followed by 93 kPa run pressure). The initial oven temperature was 50°C, followed by an immediate ramp of 26°C/min to 200°C, and a final ramping to 230°C at 2.7°C/min (hold for 11.12 min) to give a total runtime of 28

min. FAME's where detected by a flame ionization detector kept at 240°C operated in constant makeup mode. Quantification and retention time identification was achieved by external standard calibration using a five point dilution series of certified Supelco 37 component FAME mix standard (Supelco, Sigma-Aldrich) containing 37 FAME standards from C4:0 to C24:6 methylated fatty acids. Retention time confirmation and unknown peak identification were perfomed under the same capillary column and GC conditions, but using a quadropole mass selective detector (Agilent 5975) operated in SCAN EI mode (scan range 35 to 400 amu at 70 eV) and a source and quad temperature of 180 and 150°C, respectively. Unknown peaks and standard peak eluation order verification were done by identification using NIST library comparison (Agilent NIST bundle version 05).

Recovery and quality control

Matrix recovery was determined by addition of a known amount of commercial olive oil (31.86 mg) to three replicates of SNJ 25-100 µm fraction sample. Results showed a stable sample matrix recovery of 70 ± 2 % for FAME determination, and 86 ± 1 % for gravimetric determination of oil and fats. All sample analytical results were compensated using these recovery factors. A quality standard of 2 mg lipids sample using commercial olive oil, was prepared and used for analytical stability and recovery checks. External calibration standards were co-analyzed with samples to correct for retention time drifting and FID response factor compensation.

C. Solids and nutrient content in wastewater

Concentrations of total COD, TSS, VSS, ammonia, nitrate and phosphate in Vik and Mekjarvik WW are provided in table C1.

Table C1: Concentrations of total COD, TSS, VSS, ammonia, nitrate and phosphate in Vik and Mekjarvik WW (± standard error)

	Vik WW	Mekjarvik WW
COD	1421 ± 58	690 ± 30
TSS (mg L^{-1})	371 ± 4	262 ± 13
VSS (mg L^{-1})	343 ± 4	222 ± 10
NH$_4^+$ (mg N L^{-1})	30.3 ± 0.3	22.7 ± 0.5
NO$_3^-$ (mg N L^{-1})	< 0.5	< 0.5
PO$_4^{3-}$ (mg P L^{-1})	5.70 ± 0.06	2.53 ± 0.03

D. Correlations of total-N, total-P and chemical components

Nitrogen and phosphorous content of COD was compared with carbohydrate, proteinaceous material, total oils and fats, total lipids and free fatty acids, and unidentified COD by testing for correlations based on Pearson product-moment correlation coefficients (table D1). For this analysis, ammonia and phosphate concentrations was substracted from total-N and total-P data for raw WW and for the < 1 kDa fraction.

Table D1: Correlation between proteinaceous material, carbohydrate, total oils and fats, total lipids and free fatty acids and unidentified COD content (%) with total-N (TN/COD) and total-P (TP/COD) content. Correlations based on Pearson product-moment correlation coefficients, correlations are considered significant if P-values < 0.05

	Vik WW			Mekjarvik WW		
	Correlation Coefficient	**P-value**	**Significant**	**Correlation Coefficient**	**P-value**	**Significant**
Carbohydrate vs total-N	-0.28	0.4	No	0.66	0.03	Yes
Proteinaceous material vs total-N	0.84	0.009	Yes	0.84	0.001	Yes
Total oils and fats vs total-N	0.38	0.3	No	-0.16	0.6	No
Total lipids and free fatty acids vs total-N	0.24	0.5	No	0.46	0.2	No
Unidentified vs total-N	-0.18	0.6	No	-0.42	0.2	No
Carbohydrate vs total-P	-0.22	0.5	No	0.64	0.03	Yes
Proteinaceous material vs total-P	0.92	0.001	Yes	0.79	0.004	Yes
Total oils and fats vs total-P	0.78	0.008	Yes	-0.20	0.6	No
Total lipids and free fatty acids vs total-P	0.69	0.03	Yes	0.60	0.05	Yes
Unidentified vs total-P	-0.30	0.4	No	-0.33	0.3	No

E. First order simulation of BOD

For Vik WW, biological oxygen demand (BOD) was measured over 7 days for raw WW and 14 days for all size fractions (figure E1). For Mekjarvik WW, BOD was measured over 21 days for all samples (figure E1). Modelling BOD curves using first order kinetics generally has its limitations due to the models inability to follow complex degradation patterns. Especially for large particulate fractions with slower initial degradation and a distinct bimodal growth phase, the first order model gave a bad fit (figure E1). Bimodal growth was a result of initial fast growth of readily degradable particles, followed by degradation of slowly degradable particles. Bimodal growth was also observed in the smaller size fractions, however these had a faster initial growth, followed by a slower second growth period. However, for most fractions the first order model will reach a representable ultimate BOD level, thus a representable inert fraction was estimated.

The second growth phase observed in several fractions after 12 days for Vik WW and 15 days for Mekjarvik WW (figure E1) were most likely due to nitrification. No nitrification inhibitor was used during BOD tests due to possible degradation of the inhibitor itself, which would lead to interference with the BOD measurements. This is normally checked using parallel controls, but limited instrumental capacity did not allow for this in this experiment. The smaller size fractions have a late second growth phase, and in general has a lower COD/TN ratio than the particulate fractions (figure 2). On the contrary, the 10-100 kDa fraction of Mekjarvik WW had a very high COD/TN ratio and does not have a second growth phase further supporting this to be an effect of nitrification.
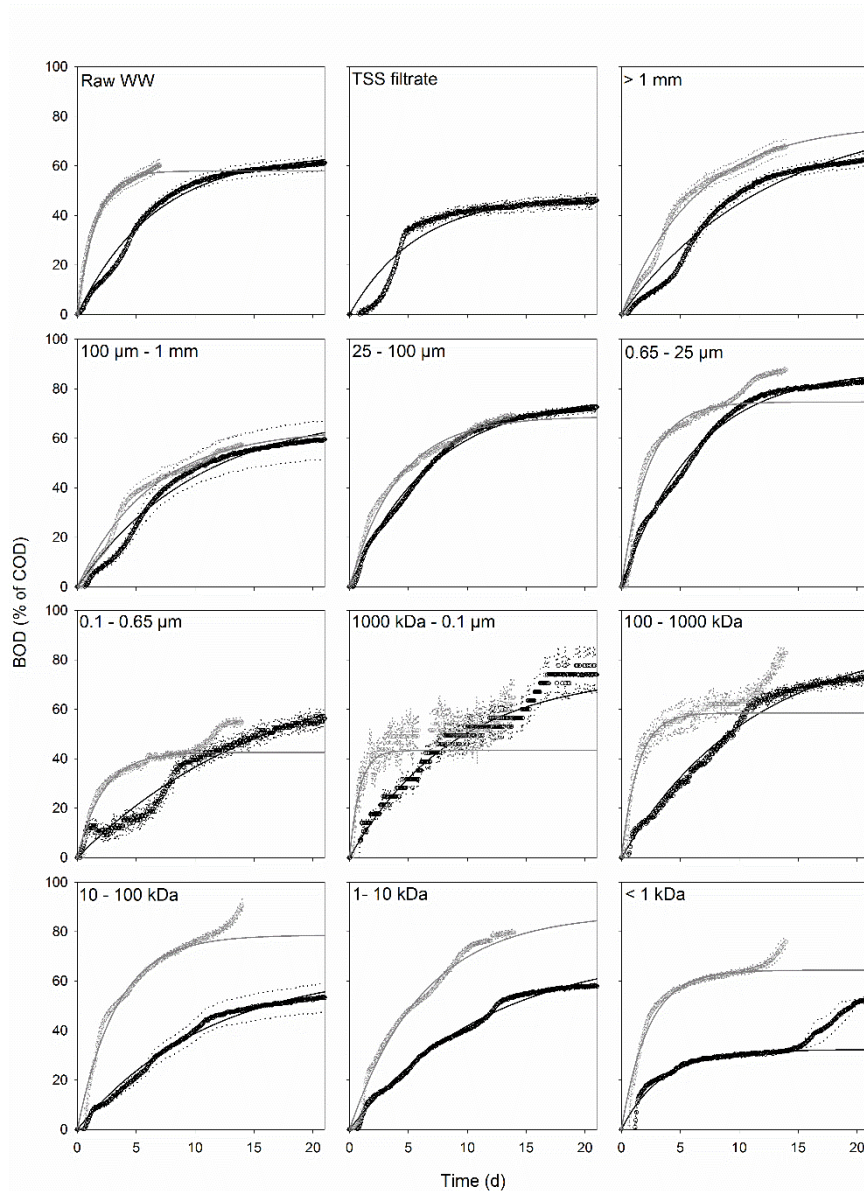
Figure E1: BOD as % of initial COD value for Vik WW (grey) and Mekjarvik WW (black). Dotted lines show standard deviations calculated for relative values, and solid lines show 1.order simulation of BOD data modelled after Roeleveld and van Loosdrecht (2002). *) 1000 kDa – 0.1 µm and 100-1000 kDa fraction data from Mekjarvik WW from one parallel only.

Inert COD fractions was estimated based on the method proposed by Roeleveld and van Loosdrecht (2002). First order kinetics was used to estimate ultimate biodegradable COD (BCOD). Inert COD was then calculated by subtracting BCOD from initial COD.

Estimated first order rate constants (k_1) and estimated fraction of inert COD (f_{inert}) are presented in table E1.

Table E1: Estimated first order rate constants (k_1) and estimated fraction of inert COD in Vik and Mekjarvik WW. Estimations based on method proposed by Roeleveld and van Loosdrecht (2002).

Fraction	Vik WW		Mekjarvik WW	
	k_1	f_{inert}	k_1	f_{inert}
	(h^{-1} mg COD^{-1})	(mg COD mg COD^{-1})	(h^{-1} mg COD^{-1})	(mg COD mg COD^{-1})
Raw WW	0.0033 ± 0.008	0.356 ± 0.002	0.00148 ± 0.00007	0.277 ± 0.009
TSS filtrate	n.a.	n.a.	0.0034 ± 0.0002	0.46 ± 0.01
> 1 mm	0.00078 ± 0.00005	0.146 ± 0.009	0.00075 ± 0.00006	0.08 ± 0.02
100 µm – 1 mm	0.00080 ± 0.00006	0.29 ± 0.02	0.0010 ± 0.0001	0.204 ± 0.008
25 – 100 µm	0.00155 ± 0.00006	0.24 ± 0.01	0.00146 ± 0.00002	0.14 ± 0.01
0.65 – 25 µm	0.00238 ± 0.00006	0.17 ± 0.01	0.00159 ± 0.00001	0.025 ± 0.004
0.1 – 0.65 µm	0.00304 ± 0.00007	0.53 ± 0.01	0.0028 ± 0.0003	0.10 ± 0.06
1000 kDa – 0.1 µm	0.065 ± 0.006	0.52 ± 0.03	0.0026*	0.17*
100 – 1000 kDa	0.0172 ± 0.0007	0.35 ± 0.04	0.0011*	0.00*
10 – 100 kDa	0.00154 ± 0.00004	0.127 ± 0.009	0.0009 ± 0.0001	0.27 ± 0.02
1 – 10 kDa	0.00080 ± 0.00001	0.03 ± 0.02	0.00084 ± 0.00004	0.18 ± 0.03
< 1 kDa	0.00229 ± 0.00004	0.284 ± 0.009	0.0029 ± 0.0002	0.64 ± 0.01

*) data from one parallel

F. Lipids concentrations

Relative concentrations of lipids in Vik wastewater (table F1) and Mekjarvik wastewater (table F2) are calculated as percentage of total lipid concentration in the size fraction.

Table F1: Relative concentration of lipids in Vik wastewater (%)

|	Raw	> 1 mm	100 μm – 1 mm	25 – 100 μm	0.65 – 25 μm	0.1 – 0.65 μm	1000 kDa – 0.1 μm	100 – 1000 kDa	10 – 100 kDa	1 – 10 kDa	< 1 kDa
C6:0	0.00	0.00	0.00	0.00	0.96		0.00	0.00	0.00	0.00	0.00
C8:0	0.00	0.00	0.00	0.00	0.89		0.00	0.00	0.00	0.00	0.00
C9:0	0.00	0.00	0.00	0.00	0.10		0.00	0.00	0.00	0.00	0.00
C10:0	0.00	0.00	0.00	0.00	2.25		0.00	0.00	0.00	0.00	0.00
C11:0	0.00	0.14	0.00	0.00	0.05		0.00	0.00	0.00	0.00	0.00
C12:0	0.42	1.92	0.00	0.85	4.21		0.00	0.00	0.00	0.00	0.00
C13:0	0.00	0.00	0.00	0.00	0.10		0.00	0.00	0.00	0.00	0.00
C14:0	6.93	5.78	3.43	6.55	12.37		0.00	0.00	0.00	0.00	0.00
C14:1	0.82	1.38	0.82	0.96	0.99		0.00	0.00	0.00	0.00	0.00
C15:0	1.02	0.61	0.70	0.88	0.06		0.00	0.00	0.00	0.00	0.00
C15:1	0.00	0.24	0.00	0.26	0.28		0.00	0.00	0.00	0.00	0.00
C16:0	39.52	29.75	27.99	31.91	36.91		11.73	5.63	10.42	30.63	0.00
C16:1	2.34	2.84	4.17	4.28	1.91		0.00	0.00	2.39	37.10	0.00
C17:0	0.52	0.55	0.92	1.32	0.70		8.46	0.00	0.00	0.00	0.00
C17:1	0.00	0.00	0.00	0.00	0.31		0.00	0.00	0.00	0.00	0.00
C18:0	17.19	19.44	16.35	17.30	13.04		25.06	15.72	17.91	9.62	0.00
C18:1n9	30.21	24.15	32.40	28.06	23.10		3.38	1.46	0.37	0.00	0.00
C18:2n6	0.47	6.83	8.59	2.84	0.08		0.00	0.00	0.00	0.00	0.00
C18:3n6	0.00	0.22	0.00	0.50	0.03		0.00	0.00	0.00	0.00	0.00
C18:3n3	0.55	2.98	1.67	0.57	0.17		0.00	0.00	0.00	0.00	0.00
C20:0	0.00	0.56	0.95	0.71	0.29		5.92	38.19	35.90	22.65	0.00
C20:1	0.00	0.23	0.00	0.17	0.20		2.68	35.61	33.00	0.00	0.00
C20:2	0.00	0.00	0.00	0.00	0.03		0.00	0.00	0.00	0.00	0.00
C20:3n6	0.00	0.00	0.00	0.00	0.08		0.00	0.00	0.00	0.00	0.00
C20:4n6	0.00	0.00	0.00	0.00	0.04		0.00	0.00	0.00	0.00	0.00
C21:0	0.00	0.00	0.00	0.00	0.04		0.00	0.00	0.00	0.00	0.00
C20:3n3	0.00	0.00	0.00	0.00	0.07		0.00	0.00	0.00	0.00	0.00
C20:5n3	0.00	0.00	0.00	0.84	0.06		0.00	0.00	0.00	0.00	0.00
C22:0	0.00	0.49	0.00	0.59	0.16		0.00	0.00	0.00	0.00	0.00
C22:1n9	0.00	0.00	0.00	0.00	0.02		0.00	0.00	0.00	0.00	0.00
C22:2	0.00	0.00	0.00	0.00	0.00		0.00	0.00	0.00	0.00	0.00
C23:0	0.00	1.90	2.01	1.41	0.38		0.00	3.39	0.00	0.00	0.00
C22:6n3	0.00	0.00	0.00	0.00	0.00		42.77	0.00	0.00	0.00	0.00
C24:0	0.00	0.00	0.00	0.00	0.11		0.00	0.00	0.00	0.00	0.00
C24:1	0.00	0.00	0.00	0.00	0.00		0.00	0.00	0.00	0.00	0.00

Table F2: Relative concentration of lipids in Mekjarvik wastewater (%)

	Raw	> 1 mm	100 µm – 1 mm	25 – 100 µm	0.65 – 25 µm	0.1 – 0.65 µm	1000 kDa – 0.1 µm	100 – 1000 kDa	10 – 100 kDa	1 – 10 kDa	< 1 kDa
C6:0	0.00	0.00	0.00	0.00	0.11	0.00	0.00	0.00	0.00	0.00	0.00
C8:0	0.00	0.00	0.00	0.00	0.20	0.00	0.00	0.00	0.00	0.00	0.00
C9:0	0.00	0.25	0.00	0.00	0.18	0.00	0.00	0.00	0.00	0.00	0.00
C10:0	0.00	0.08	0.00	0.00	0.66	0.00	0.00	0.00	0.00	0.00	0.00
C11:0	0.00	0.00	0.00	0.00	0.00	0.00	0.00	0.00	0.00	0.00	0.00
C12:0	0.00	1.30	0.00	1.09	2.36	0.00	0.00	0.00	0.00	4.93	0.00
C13:0	0.00	0.00	0.00	0.00	0.04	0.00	0.00	0.00	0.00	0.00	0.00
C14:0	19.64	3.17	2.14	3.43	6.48	0.00	0.00	0.00	0.00	0.00	0.00
C14:1	0.00	1.91	0.68	1.09	0.83	0.00	0.00	0.00	0.00	8.40	0.00
C15:0	0.00	0.54	0.45	0.70	1.00	0.00	0.00	0.00	0.00	0.00	0.00
C15:1	0.00	0.20	0.00	0.24	0.27	0.00	0.00	0.00	0.00	0.00	0.00
C16:0	21.30	25.55	21.40	25.74	30.39	35.89	4.84	0.00	17.46	14.54	0.00
C16:1	2.49	2.97	1.97	3.40	3.00	0.00	17.49	0.00	0.00	0.00	0.00
C17:0	0.00	0.67	0.34	1.03	0.93	0.00	0.00	0.00	0.00	0.00	100.00
C17:1	0.00	0.18	0.00	0.00	0.27	0.00	0.00	0.00	0.00	0.00	0.00
C18:0	19.99	15.66	16.87	20.22	22.29	64.11	13.90	0.00	49.95	0.00	0.00
C18:1n9	28.72	40.41	32.82	27.64	26.90	0.00	3.28	0.00	32.58	0.00	0.00
C18:2n6	7.88	0.15	9.99	8.80	0.24	0.00	0.00	0.00	0.00	0.00	0.00
C18:3n6	0.00	0.07	0.00	0.28	0.11	0.00	0.00	0.00	0.00	0.00	0.00
C18:3n3	0.00	0.16	1.10	1.09	0.22	0.00	0.00	0.00	0.00	0.00	0.00
C20:0	0.00	0.71	0.84	0.87	0.72	0.00	60.50	59.99	0.00	0.00	0.00
C20:1	0.00	0.77	7.89	0.51	0.44	0.00	0.00	40.01	0.00	0.00	0.00
C20:2	0.00	0.00	0.00	0.00	0.00	0.00	0.00	0.00	0.00	0.00	0.00
C20:3n6	0.00	0.00	0.00	0.00	0.00	0.00	0.00	0.00	0.00	0.00	0.00
C20:4n6	0.00	0.00	0.00	0.00	0.00	0.00	0.00	0.00	0.00	0.00	0.00
C21:0	0.00	0.00	0.00	0.00	0.00	0.00	0.00	0.00	0.00	0.00	0.00
C20:3n3	0.00	0.00	0.76	0.00	0.00	0.00	0.00	0.00	0.00	72.13	0.00
C20:5n3	0.00	0.00	0.00	0.00	0.00	0.00	0.00	0.00	0.00	0.00	0.00
C22:0	0.00	0.73	0.74	0.74	0.56	0.00	0.00	0.00	0.00	0.00	0.00
C22:1n9	0.00	0.23	0.00	0.00	0.00	0.00	0.00	0.00	0.00	0.00	0.00
C22:2	0.00	0.00	0.00	0.00	0.00	0.00	0.00	0.00	0.00	0.00	0.00
C23:0	0.00	3.85	1.99	2.64	1.43	0.00	0.00	0.00	0.00	0.00	0.00
C22:6n3	0.00	0.00	0.00	0.00	0.00	0.00	0.00	0.00	0.00	0.00	0.00
C24:0	0.00	0.45	0.00	0.49	0.37	0.00	0.00	0.00	0.00	0.00	0.00
C24:1	0.00	0.00	0.00	0.00	0.00	0.00	0.00	0.00	0.00	0.00	0.00

G. SEC-MALS-dRI data

This sections contains additional SEC-MALS-dRI data for comparison. Fractions > 0.65 µm not included. Note the wide distributions and lack of adequate separation (complete exclusion) for fractions larger than ~1000kDa. Note the unexpected peak shape of the > 0.65 µm fraction, indicating a cut-off due to the filtration of sample prior to injection. SEC-MALS-dRI data for > 0.65 µm fraction is therefore not included in the dataset.

Fraction	Mw (kDa)	Uncertainty Mw	Rz (nm)	Uncertainty Rz	Conc. from dRI (mg L^{-1})
> 1kDa	35	35 %	-	-	35
> 10 kDa	260	22 %	-	-	48
> 100 kDa	1164	19 %	47	72 %	27
> 1000 kDa	13203	57 %	162	22 %	5
> 0.1 µm	-	-	335	7 %	13
> 0.65 µm	-	-	-	-	-
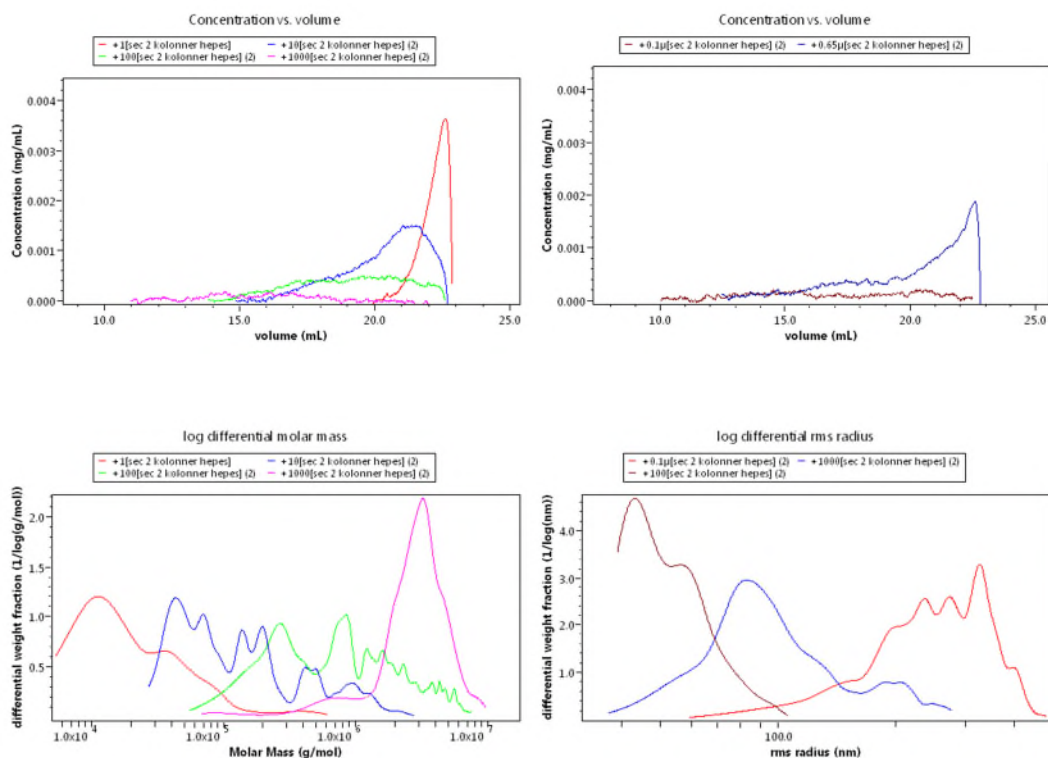
References

Roeleveld, P.J., van Loosdrecht, M.C.M. 2002. Experience with guidelines for wastewater characterisation in The Netherlands. *Water Science and Technology*, **45**(6), 77-87.

Ryckebosch, E., Muylaert, K., Foubert, I. 2012. Optimization of an analytical procedure for extraction of lipids from microalgae. *Journal of the American Oil Chemists' Society*, **89**(2), 189-198.